Polymer Chemistry

Accepted Manuscript

ROYAL SOCIETY OF CHEMISTRY

www.rsc.org/polymers

The table of contents entry:

Fluorinated low band gap copolymer based on dithienosilole-benzothiadiazole for high-performance photovoltaic device

Hongying Lv,[abc] Xiaoli Zhao,[ab]* Zidong Li,[abc] Dalei Yang,[abc] Zhongliang Wang,[ad] and Xiaoniu Yang[ab] *

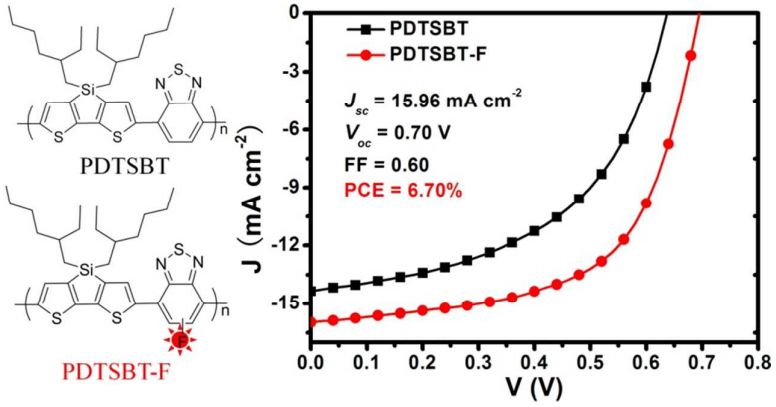

The introduction of fluorine atom onto a copolymer of dithienosilole-benzothiadiazole brings significant enhancement in PSCs with a PCE increased from 4.68% to 6.70%.

Fluorinated low band gap copolymer based on dithienosilole-benzothiadiazole for high-performance photovoltaic device

Hongying Lv,[abc] Xiaoli Zhao,[ab] * Zidong Li,[abc] Dalei Yang,[abc] Zhongliang Wang,[ad] and Xiaoniu Yang[ab] *

[a]Polymer Composites Engineering Laboratory, Changchun Institute of Applied Chemistry, Chinese Academy of Sciences, Renmin Str. 5625, Changchun 130022, P. R. China

[b]State Key Laboratory of Polymer Physics and Chemistry, Changchun Institute of Applied Chemistry, Chinese Academy of Sciences, Renmin Str. 5625, Changchun 130022, P. R. China

[c]University of Chinese Academy of Sciences, Beijing 100049, P. R. China

[d]Changchun University of Technology, Changchun 130012, P.R. China

* Correspondence to: X.N. Yang (E-mail: xnyang@ciac.jl.cn); X.L. Zhao (E-mail: zhaoxiaoli@ciac.jl.cn)

Abstract

A new fluorinated low band gap copolymer, poly[(4,4'-bis(2-ethylhexyl)dithieno[3,2-b:2',3'-d]silole)-2,6-diyl-alt-4,7-(5-fluoro-2,1,3-benzothiadiazole)] (PDTSBT-F) was designed and synthesized. The introduction of fluorine atom onto a classical low band gap copolymer (PDTSBT) has a little influence on the polymer absorption spectrum and band gap, which was 1.48 eV for PDTSBT-F. However, the HOMO level was lowered to -5.17 eV for PDTSBT-F, the film crystallinity was improved, and PDTSBT-F showed higher charge carrier mobility than the non-fluorinated analogue (PDTSBT). For the PDTSBT-F/$PC_{71}BM$ device, a J_{sc} of 15.96 mA cm^{-2}, a V_{oc} of 0.70 V, and a FF of 0.60 were attained, resulting in a PCE of 6.70%, to the best of our knowledge, which is the highest value to date in the devices based on copolymers with C-, Si- and Ge-bridged dithiophene as the electron-rich unit and benzothiadiazole derivatives as electron-deficient unit. A high PCE in combination with a wide absorption spectrum in the visible range could induce PDTSBT-F to be a potentially promising low band gap polymer for polymer solar cells.

Introduction

Polymer solar cells (PSCs) as a renewable energy source have been gaining more and more attention owing to their potential of low cost, light weight and large-area fabrication.[1-4] Significant improvement in device performance has been achieved in the past years through developing photovoltaic materials,[5-6] interfacial layer,[7-9] and device architecture.[10-11] D-A copolymers composed of alternant electron-rich unit (D) and electron-deficient unit (A) are widely employed as electron donor materials for high efficiency PSCs. This rational design concept has been confirmed to be effective in tuning the band gap, energy levels and hole mobility of polymers.[6, 12-15] Among these polymers, poly[(4,4′-bis(2-ethylhexyl)dithieno[3,2-b:2′,3′-d]silole)-2,6-diyl-alt-(2,1,3-benzothiadiazole)-4,7-diyl] (PDTSBT) has been attracting more interest as a potentially high efficient donor material because of its wide absorption response in the range of 300-850 nm, which has good matching with the sun spectrum.[16-18] Many efforts including thermal annealing,[19] solvent vapor annealing,[20] inverted device geometry,[21-22] and optimizing alkyl chain[23] have been made towards improving the PDTSBT-based photovoltaic performance. However, the low open circuit voltage (V_{oc}) significantly limits the power conversion efficiencies (PCEs) for PDTSBT-based device, where [6,6]-phenyl-C71-butyric acid methyl ester ($PC_{71}BM$) acts as electron acceptor material. Therefore, further improvement in efficiency of PDTSBT-based device is expected to be attained through increasing V_{oc}, while maintaining the high short current density and fill factor. Raising lowest unoccupied molecular orbital (LUMO) level of acceptor or lowering highest occupied molecular orbital (HOMO) level of donor is an effective way to increase the V_{oc}.[24-26] One of fullerene derivatives with high-lying LUMO level, indene-C60 bisadduct (ICBA), has been effectively

employed in devices based on poly(3-hexylthiophene) (P3HT), while it rarely brings good performance in the low band gap polymer-based devices, and has adverse effect on the PDTSBT-based device.[25, 27-29] Thus, lowering the HOMO level of PDTSBT could be a better alternative method to increase the V_{oc} and then the device performance.

Recently, the application of fluorine atom, as an electron-withdrawing group on the polymer backbone, has attracted more interest due to the ability of simultaneously lowering the HOMO and LUMO levels, having a little effect on the polymer band gap and thus enhancing the V_{oc}.[6, 13, 15, 26, 30-31] Meanwhile, the size of fluorine atom is similar to the hydrogen atom, which would not introduce additional steric hindrance; and its strong electronegativity could increase intra- and intermolecular interaction through F···H, F···S interaction, which may be favorable for the polymer self-assembly and improve the crystallinity. Moreover, the oligomeric DTS-fluorinated-BT compound as a donor material shows interesting photovoltaic performance,[32] which makes copolymer based on DTS-fluorinated-BT more appealing. Based on this strategy, it may be an effective way of enhancing the device performance based on the classical low band gap copolymer PDTSBT by adding fluorine atom on the polymer chain.

In this work, we synthesized a new partially fluorinated low band gap copolymer, poly[(4,4'-bis(2-ethylhexyl)dithieno[3,2-b:2',3'-d]silole)-2,6-diyl-alt-4,7-(5-fluoro-2,1,3-benzothiadiazole)] (PDTSBT-F), which was formed by copolymerizing monofluoro-substituted benzothiadiazole unit with dithienosilole unit. Effect of fluorination on the optical, electrochemical, crystallinity, charge carrier mobility and photovoltaic properties of PDTSBT-F were investigated, and the non-fluorinated analogue PDTSBT was also studied for comparison. It is interesting that the device PCE was significantly increased from 4.68% for PDTSBT/$PC_{71}BM$

blend to 6.70% for PDTSBT-F/$PC_{71}BM$ blend, which indicates PDTSBT-F could be a promising low band gap candidate for the photovoltaic devices.

Results and discussion

Polymer Synthesis and Characterization

The synthetic routes of the monomers and polymers are shown in Scheme 1. The preparation of the 4,4'-bis(2-ethylhexyl)-5,5'-bis(trimethyltin)-dithieno[3,2-b:2',3'-d]silole and 4,7-dibromo-5-fluoro-2,1,3-benzothiadiazole were performed similarly to previous literature.[16, 33] Compound M2 was prepared by N-bromosuccinimide (NBS) bromination via electrophilic substitution to replace the trimethylsilyl moiety which acted as protecting group. Lithiation of compound M2 with n-butyllithium (n-BuLi) followed by quenching with trimethyltin chloride to afforded M3. Compound M3 was difficult to be purified by recrystallization or column chromatography, and it was directly copolymerized with the electron-deficient units to generate the corresponding copolymers via a modified Stille coupling reaction with $Pd_2(dba)_3$ as catalyst and $P(o\text{-tolyl})_3$ as the ligand. In order to achieve high molecular weights, a stoichiometric ratio of 1.04:1.00 (compound M3 to the corresponding acceptor monomers) was applied in the reaction with the intention of compensating for possible contamination of M3 resulting from organometallic tin compounds. The crude copolymers were purified by reprecipitation and Soxhlet extraction to remove oligomers and residual catalyst. The number average molecular weights (M_n) of polymers were measured by GPC in 1,2,4-trichlorobenzene (TCB) at 150 ^oC with polystyrene as standards. The M_n for PDTSBT-F was 16 000 g mol^{-1} with a PDI of 1.78, while the M_n of PDTSBT was 22 000 g mol^{-1} with a PDI of 2.38 (Figure S1 in Supporting Information). The thermal stabilities of PDTSBT-F and PDTSBT were investigated by thermogravimetric analysis

(TGA), and the decomposition temperatures (5% weight loss) were 420 and 440 ^{o}C for PDTSBT-F and PDTSBT (Figure S2), respectively, indicating both copolymers have good thermal stability.

Optical and Electrochemical properties

The UV-vis absorption spectra of PDTSBT-F and PDTSBT were measured in CB solutions and in thin films. As shown in Figure 1a, both polymers in hot solutions (90 ^{o}C) showed similar absorption characteristic with a main absorption peak at around 670 nm, which may be due to the similar polymer backbone. For PDTSBT-F solution, there was a weak shoulder peak at about 730 nm, which could be attributed to the π-π interaction of polymer chains,[16, 19] indicating intermolecular interaction of PDTSBT-F in solution was slightly increased. When both solutions were cooled to the room temperature, an obvious red-shift of the main peak was observed from 670 to 690 nm, which implies the polymer chains showed high planarity compared to that in hot solution. Meanwhile, the π-π interaction peak was found in both polymer solutions with a slight blue-shift of about 10 nm for PDTSBT-F solution (730 nm) compared to that of PDTSBT solution (740 nm). The intensity of π-π interaction peak in PDTSBT-F was slightly higher than that of PDTSBT, which is consistent with the result in hot solutions. Figure 1b exhibits the absorption spectra of both polymers in films. In comparison with the absorption of polymer solutions, the π-π interaction peak in both films became intense and red-shifted with peaks at 750 nm for PDTSBT-F and 760 nm for PDTSBT, respectively, which implies more enhanced intermolecular interaction or ordered structures in the solid state. The slightly stronger intensity of π-π interaction peak in PDTSBT-F confirms improved intermolecular interaction by the addition of fluorine atom, which was also observed in other fluorinated copolymers.[13, 15] An optical band gap of 1.48 eV for PDTSBT-F was determined from the film absorption onset, which was similar to that of PDTSBT

(1.46 eV). It is worthy to note that the absorption spectrum and optical band gap of the new polymer PDTSBT-F were very similar to those of the nonfluorinated analogue PDTSBT, indicating the introduction of fluorine atom on the copolymer chain has a little effect on the band gap and absorption spectra. The absorption characteristics of both polymers are listed in Table 1.

Cyclic voltammetry was employed to study electrochemical properties and determine the HOMO and LUMO energy levels of both polymers as thin films. The potential of calomel reference electrode was internally calibrated by using ferrocene/ferrocenium (Fc/Fc^{+}) redox couple. The oxidation/reduction onsets of polymers were determined at the position where the current began to differ from the baseline. Cyclic voltammogram of PDTSBT-F and PDTSBT are shown in Figure 2, and the corresponding data are summarized in Table 1. The reduction onsets potentials (E_{onset}^{red}) of PDTSBT-F and PDTSBT were -1.54 V and -1.60V versus Fe/Fe^{+}, respectively, while the oxidation onset potentials (E_{onset}^{ox}) were 0.37 V and 0.2 V versus Fe/Fe^{+}, respectively. The HOMO and LUMO energy levels as well as the energy gap of the polymers were calculated from the onset of the oxidation potential and reduction potential according to the equations: $HOMO = -eV(E_{onset}^{ox} + 4.8)$, $LUMO = -eV(E_{onset}^{red} + 4.8)$ and $E_g^{EC} = eV(E_{onset}^{ox} - E_{onset}^{red})$. The estimated HOMO energy levels were -5.17 eV for PDTSBT-F and -5.00 eV for PDTSBT, while the estimated LUMO levels of PDTSBT-F and PDTSBT were -3.26 eV and -3.20 eV, respectively. It can be found that the HOMO level was significantly decreased from -5.00 eV to -5.17 eV by changing the electron-deficient unit from benzothiadiazole to monofluoro-substituted benzothiadiazole, and the LUMO level only lowered from -3.20 eV to -3.26 eV. The result indicates that introducing fluorine atom onto PDTSBT could reduce the LUMO and HOMO levels in different degrees, and this difference between HOMO and LUMO

decrease degree results in the slightly increased band gap in PDTSBT-F. The deeper HOMO energy level is desirable for higher V_{oc}, since the V_{oc} is proportional to the difference between the HOMO level of donor material and the LUMO level of acceptor material. The eventual efficiency of the devices is the trade off of the band-gap and V_{oc}, while maintaining sufficient LUMO-LUMO offset of the donor and acceptor materials.

Crystallinity and Charge transporting properties of polymers

To investigate the effect of fluorination on the crystallinity of polymers, the out-of-plane X-ray diffraction (XRD) was carried out for PDTSBT-F and the nonfluorinated analogue (PDTSBT) films. As shown in Figure 3, both polymers showed a diffraction peak at 2θ of around 5.3° (16.66 Å), which was attributed to the reflection of (100) planes, i.e. the lamellar packing.[19, 34] It is noticed that a weak π-π stacking peak at 2θ of around 25.2° (3.53 Å) existed in PDTSBT, which was so broad and weak that its contribution to the crystallinity could be neglected. For PDTSBT-F, there was no obvious shift for the position of (100) diffraction peak, which indicates that the fluorine atom on polymer chain likely has little influence on the spacing of the lamellar packing. This may be due to the similar size of fluorine and hydrogen atom, which would not lead to additional steric hindrance in the lamellar packing. However, the intensity of the lamellar packing in the PDTSBT-F film was much stronger than that of PDTSBT film, which reflects the increased crystallinity in the PDTSBT-F film. Taking difference between PDTSBT-F and PDTSBT into account, we suggest that the significant improvement in crystallinity of PDTSBT-F film may benefits from the noncovalent F-H, F-F interactions of fluorinated polymer chains.

The hole mobility (μ_h) of polymer films was measured by space charge limited current (SCLC) method to investigate the charge carrier transport in PDTSBT-F and PDTSBT films. The

fabrication procedure is described in the experimental section. Figure 4a exhibits the hole-only dark *I-V* curves of both polymer films, in which the hole-only current of PDTSBT-F film was higher than that of PDTSBT film. The SCLC hole mobility was estimated by fitting the hole-only *I-V* curves with SCLC model and the Mott-Gurney law:

$$\ln(I / V^2) = 0.89\beta(V / L)^{1/2} + \ln(9\mu\varepsilon_0\varepsilon S / (8L^3)) \qquad (1)$$

where I is the current, V is the applied voltage, β is the field-activation factor, L is the thickness of polymer film, μ is the mobility, ε_0 is the permittivity of free space, ε is the relative permittivity, and S is the area of polymer film.[20, 35-36] Figure 4b shows the linear fits for the plots of $\ln(I / V^2)$ versus $V^{1/2}$ of both polymers, which is based on the SCLC model, and the results are summarized in Table 1. The μ_h of PDTSBT-F was 1.09×10^{-4} cm^2 V^{-1} s^{-1}, which was almost two times higher than that of PDTSBT ($\mu_h = 5.54 \times 10^{-5}$ cm^2 V^{-1} s^{-1}). This result indicates the addition of fluorine atom on polymer chain is favorable for charge carrier mobility, meanwhile, implies effective charge carrier transportation for the vertically structured device based on PDTSBT-F.

Bulk Heterojunction Photovoltaic Device Performance

With similar band gap, deeper HOMO level and enhanced film crystallinity for PDTSBT-F relative to PDTSBT, the BHJ photovoltaic device employing PDTSBT-F as donor would be expected to be better than that of PDTSBT. The devices were fabricated with the configuration of ITO/PEDOT:PSS /polymer:$PC_{71}BM$/Ca /Al. The performance of PDTSBT-F-based devices was optimized by the ratio of donor and acceptor, addition of additive (1,8-diiodoctane (DIO)), and thermal annealing treatment. *J-V* curves of the devices under different processing condition are exhibited in Figure S3 and the corresponding performance characteristics are listed in Table S1. The optimized device was processed from PDTSBT-F:$PC_{71}BM$ (1:1.5, w:w) solution containing 1

vol % DIO, and thermal annealed at 80 ^{o}C for 10 min. Figure 5a shows *J-V* curve of the optimized PDTSBT-F-based device and that of PDTSBT for comparison. The photovoltaic performance of corresponding devices is listed in Table 2. The PSCs made from PDTSBT showed a PCE of 4.68%, which was comparable with the literature.[16, 20] In contrast, the device based on PDTSBT-F exhibited a significantly improved PCE of 6.70% with a J_{sc} of 15.96 mA cm^{-2}, a V_{oc} of 0.70 V, and a FF of 0.60. Meanwhile, the external quantum efficiency (EQE) of devices based on both polymers was investigated in atmosphere. As shown in Figure 5b, both devices exhibited broad photo-to-current response in the range of 300-850 nm. The EQE of device based on PDTSBT-F was higher than that of PDTSBT-based device from 300 to 770 nm, which agrees with the higher J_{sc} in PDTSBT-F device. The integrated J_{sc} values from EQE curves are consistent with the measured J_{sc} within 7% deviation, which may be due to the oxidation of Ca layer in atmosphere and the possible mismatch between simulated sun light and AM 1.5G solar spectrum. These PCE and EQE results indicate the device performance based on dithienosilole-benzothiadiazole copolymer can be effectively improved by the addition of fluorine atom to the copolymer chain.

The enhancement in PCE of PDTSBT-F-based device apparently results from simultaneous increase in J_{sc}, V_{oc} and FF. The improved V_{oc} (0.06 V) was attributed to the deeper HOMO level of PDTSBT-F than that of PDTSBT, while the enhancement in J_{sc} and FF could be ascribed to the suppressed charge recombination by introducing the fluorine substituent,[37-38] and the improved crystallinity of PDTSBT-F/$PC_{71}BM$ blend film, as shown in Figure 6, which could bring benefit to the charge carrier transport. The device performance is also dependent on the morphology of active layer, in which suitable length-scale of phase separation is favorable for high efficiency. As shown in Figure 7, the PDTSBT domains mixed well with $PC_{71}BM$ aggregates, which formed

relatively small phase separation in PDTSBT/$PC_{71}BM$ film. In comparison with that, the phase separation of PDTSBT-F/$PC_{71}BM$ film was slightly larger with obvious PDTSBT-F nanocrystallites, which may be also beneficial to efficient exciton dissociation and charge transportation. AFM images (Figure S4) also reveal slightly increased aggregation in the PDTSBT-F/$PC_{71}BM$ film. In consequence, by combing increased V_{oc}, J_{sc} and FF, a much higher PCE (6.70%) was achieved for the PDTSBT-F-based device compared to the PDTSBT-based device.

Conclusions

In this work, we have synthesized a fluorinated dithienosilole-benzothiadiazole copolymer, PDTSBT-F, by Stille polymerization. The optical, electrochemical, crystallinity, charge carrier mobility and photovoltaic properties were investigated for both PDTSBT-F and PDTSBT. It was found that the fluorine atom has a little effect on the band gap and absorption spectrum of PDTSBT-F, which was similar with that of nonfluorinated analogue (PDTSBT). However, the HOMO level was lowered from -5.00 eV for PDTSBT to -5.17 eV for PDTSBT-F, and the crystallinity was obviously improved by addition of fluorine atom on the copolymer chain, which also resulted in a almost two times higher hole mobility in PDTSBT-F compared to PDTSBT. Most importantly, the device made from PDTSBT-F/$PC_{71}BM$ showed a PCE of 6.70% with a J_{sc} of 15.96 mA cm^{-2}, a V_{oc} of 0.70 V, and a FF of 0.60. To the best of our knowledge, it is the highest PCE value to date in the devices based on copolymers with C-, Si- and Ge-bridged dithiophene as the electron-rich unit and benzothiadiazole derivatives as electron-deficient unit. The lowered HOMO level should be responsible to the increased V_{oc}, while the high J_{sc} and FF result from the improved crystallinity and morphology of PDTSBT-F/$PC_{71}BM$ film. These results indicate the

device performance based on dithienosilole-benzothiadiazole copolymer can be effectively improved by the addition of fluorine atom to the copolymer chain, and PDTSBT-F could be a promising low band gap polymer for the high efficiency solar cells.

Experimental Section

Measurements. ^{1}H-NMR spectra of polymers was recorded with a Bruker AV-400MHz spectrometer at 120 ^{o}C in 1,1,2,2-tetrachloroethane-d_2 as solvent. The molecular weight was measured by gel permeation chromatography (GPC) on a PL-GPC220 instrument. Thermogravimetric analysis (TGA) was carried out on a METTLER TOLEDO TGA/DSC1/1100 LF equipment under nitrogen and a heating rate of 10 ^{o}C min^{-1}. Differential scanning calorimetry (DSC) was measured on a TA Q100 DSC under nitrogen atmosphere and a heating and cooling rate of 10 ^{o}C min^{-1}. UV-vis absorption spectra were obtained using a Perkin-Elmer UV-vis Lambda 750 spectrometer. Electrochemical properties of both polymer films were performed on a CHI600D electrochemical analyzer in anhydrous acetonitrile at a scan rate 100 mV s^{-1} under nitrogen. Tetrakis(n-butyl)ammonium hexafluorophosphate (Bu_4NPF_6) (0.1 M) was used as electrolyte. A glassy carbon electrode, a saturated calomel electrode, and a Pt wire were used as the working, reference, counter electrodes, respectively. Polymer films were spin-coated onto the glassy carbon working electrode from a chlorobenzene solution (8 mg ml^{-1}).

XRD was determined on a Rigaku SmartLab X-ray diffractometer (Cu, λ = 1.54056 Å) with a 40kV tube voltage and 30 mA tube current. TEM was performed on a JEOL JEM-1011 transmission electron microscope operated at an acceleration voltage of 100 kV. AFM was obtained on a Bruker Nanoscope IIIA using tapping mode. J-V characteristics of the polymer photovoltaic devices were measured in a glove box with a Keithley-2400 source meter and a solar

simulator (SAN-EI, XES-70S1) at AM 1.5G illumination of 100 mW cm^{-2}. The IPCE of the devices was measured using chopped monochromatic light from an iodine tungsten lamp in atmospheric environment. A standard silicon solar cell was used as reference to determine the light intensity at each wavelength. J-V characteristics of the polymer hole-only devices were determined in a glove box in the dark with a Keithley-2400 source meter. Thickness of the films was acquired on a KLA-Tencor D-100 surface profiler.

Fabrication of Polymer Photovoltaic and Hole-only Devices. The indium tin oxide (ITO) coated glass substrates were cleaned in sequence with detergent, deionized water and isopropyl alcohol. After the ITO substrates were treated under UV ozone for 30 min, a *ca.* 30 nm PEDOT:PSS layer was spin-coated and annealed at 150 ^{o}C for 15 min. Then these substrates were transferred into a glove box. The photoactive layer of PDTSBT-based device was fabricated as described in our previous work.[20] For the PDTSBT-F devices, PDTSBT-F/$PC_{71}BM$ blend was dissolved in CB (6 mg ml^{-1} for PDTSBT-F) with different blend ratio. The solution containing different amount DIO was heated to 100 ^{o}C prior to spin-coating the photovoltaic active layer with a thickness of *ca.* 90 nm. For the hole-only devices, a ca. 50 nm polymer layer was spin-coated on the substrates from both polymer solutions, where PDTSBT-F solution was heated at 100℃ prior to spin-coating. Afterwards, the PDTSBT-F/$PC_{71}BM$ films were thermally annealed at different conditions, and the PDTSBT/$PC_{71}BM$ films were thermally annealed at 140 ^{o}C for 5 min as reported in literature.[16, 20] Finally, a 20 nm Ca layer topped with a 100 nm Al was evaporated on the active layer for the photovoltaic devices fabrication. The hole-only devices were completed by evaporation of a 90 nm Au electrode. The photoactive area of each device was 9 mm^2.

Material. All reagents, unless stated, were received from commercial sources and used without

further purification. $PC_{71}BM$ (99%) was purchased from American Dye Source Inc. Chlorobenzene (CB, anhydrous, 99%) and 1,8-diiodoctane (DIO) were purchased from Sigma-Aldrich and TCI, respectively. Toluene was dried over sodium/benzophenone and freshly distilled prior to use. The monomers of 4,4'-bis(2-ethylhexyl)-5,5'-bis(trimethyltin)-dithieno[3,2-b:2',3'-d]silole and 4,7-dibromo-5-fluoro-2,1,3-benzothiadiazole were synthesized similarly to the procedures described in previous literature.[16, 33]

Synthesis of PDTSBT-F. Compound M3 (1.2 mmol, 0.89 g) and M6 (1.15 mmol, 0.36 g) were dissolved in anhydrous toluene (10 ml) and DMF (2 ml). After being flushed with argon for 10 min, $Pd_2(dba)_3$ (0.018 mmol) and $P(o\text{-}tolyl)_3$ (0.144 mmol) were added into the solution. The mixture was again flushed with argon for another 15 min. Then the resulted solution was heated at 120 ^oC for 48 hours. After cooling to room temperature, the reaction mixture was precipitated by adding dropwise into 100 ml methanol and filtered. The precipitate was collected and subjected to Soxhlet extraction with methanol, acetone, hexane, and chloroform in sequence. The residual fraction was collected and dried in vacuum to afford a blue solid as product (220 mg, 32%). ^{1}H-NMR (400MHz, $C_2D_2Cl_4$, 120 ^oC, ppm): 8.58-8.13 (d, br, 2H), 7.82 (br, 1H), 2.71 (br, 4H), 1.96-0.70 (d, br, 30H). Molecular weight: M_n = 16 000 g mol^{-1}, PDI = 1.78.

Synthesis of PDTSBT. PDTSBT was prepared following the procedure for PDTSBT-F using M3 and benzothiadiazole as monomers. The chloroform fraction was then precipitated in 100 ml methanol, then the polymer was collected and dried in high vacuum to afford a blue solid as product (440mg, 67%).^{1}H-NMR (400MHz, $C_2D_2Cl_4$, 120 ^oC, ppm): 8.24 (br, 2H), 7.93 (br, 2H), 2.83(br, 4H), 1.98-0.67 (d, br, 30H). Molecular weight: M_n = 22 000 g mol^{-1}, PDI = 2.38.

Acknowledgements

This work was financially supported by the National Natural Science Foundation of China (Grant No. 20874100, 20925415, 20990233 and 50921062), the Solar Energy Initiative (Grant No. KGCX2-YW-399 + 9) of the Chinese Academy of Sciences, and the Hi-Tech Research and Development Program (863) of China (2011AA050524).

References

1. F. C. Krebs, *Sol. Energy Mater. Sol. Cells*, 2009, **93**, 394-412.
2. T. R. Andersen, T. T. Larsen-Olsen, B. Andreasen, A. P. L. Bottiger, J. E. Carle, M. Helgesen, E. Bundgaard, K. Norrman, J. W. Andreasen, M. Jorgensen and F. C. Krebs, *Acs Nano*, 2011, **5**, 4188-4196.
3. G. Li, R. Zhu and Y. Yang, *Nat. Photon.*, 2012, **6**, 153-161.
4. W. Li, K. H. Hendriks, W. S. C. Roelofs, Y. Kim, M. M. Wienk and R. A. J. Janssen, *Adv. Mater.*, 2013, **25**, 3182-3186.
5. T.-Y. Chu, J. Lu, S. Beaupre, Y. Zhang, J.-R. Pouliot, S. Wakim, J. Zhou, M. Leclerc, Z. Li, J. Ding and Y. Tao, *J. Am. Chem. Soc.*, 2011, **133**, 4250-4253.
6. H.-C. Chen, Y.-H. Chen, C.-C. Liu, Y.-C. Chien, S.-W. Chou and P.-T. Chou, *Chem. Mater.*, 2012, **24**, 4766-4772.
7. Z. a. Tan, W. Zhang, Z. Zhang, D. Qian, Y. Huang, J. Hou and Y. Li, *Adv. Mater.*, 2012, **24**, 1476-1481.
8. Z. He, C. Zhong, S. Su, M. Xu, H. Wu and Y. Cao, *Nat. Photon.*, 2012, **6**, 591-595.
9. K. M. O'Malley, C.-Z. Li, H.-L. Yip and A. K. Y. Jen, *Adv. Energy Mater.*, 2012, **2**, 82-86.
10. L. Yang, H. Zhou, S. C. Price and W. You, *J. Am. Chem. Soc.*, 2012, **134**, 5432-5435.
11. J. You, L. Dou, K. Yoshimura, T. Kato, K. Ohya, T. Moriarty, K. Emery, C.-C. Chen, J. Gao, G. Li and Y. Yang, *Nat. Commun.*, 2013, **4**, 1446.
12. P. M. Beaujuge and J. M. J. Frechet, *J. Am. Chem. Soc.*, 2011, **133**, 20009-20029.
13. Y. Zhang, J. Zou, C.-C. Cheuh, H.-L. Yip and A. K. Y. Jen, *Macromolecules*, 2012, **45**, 5427-5435.
14. X. Zhao, D. Yang, H. Lv, L. Yin and X. Yang, *Polym. Chem.*, 2013, **4**, 57-60.
15. M. Zhang, X. Guo, S. Zhang and J. Hou, *Adv. Mater.*, 2014, **26**, 1118-1123.
16. J. H. Hou, H. Y. Chen, S. Q. Zhang, G. Li and Y. Yang, *J. Am. Chem. Soc.*, 2008, **130**, 16144-16145.
17. S. Sista, Z. Hong, M.-H. Park, Z. Xu and Y. Yang, *Adv. Mater.*, 2010, **22**, E77-E80.
18. J. Yang, R. Zhu, Z. Hong, Y. He, A. Kumar, Y. Li and Y. Yang, *Adv. Mater.*, 2011, **23**, 3465-3470.
19. H. Y. Chen, J. H. Hou, A. E. Hayden, H. Yang, K. N. Houk and Y. Yang, *Adv. Mater.*, 2010, **22**, 371-375.
20. H. Lv, X. Zhao, W. Xu, H. Li, J. Chen and X. Yang, *Org. Electron.*, 2013, **14**, 1874-1881.
21. J. Subbiah, C. M. Amb, J. R. Reynolds and F. So, *Sol. Energy Mater. Sol. Cells*, 2012, **97**, 97-101.

22. J. Subbiah, C. M. Amb, I. Irfan, Y. Gao, J. R. Reynolds and F. So, *ACS Appl. Mater. Interfaces*, 2012, **4**, 866-870.
23. R. C. Coffin, J. Peet, J. Rogers and G. C. Bazan, *Nat. Chem.*, 2009, **1**, 657-661.
24. C. J. Brabec, A. Cravino, D. Meissner, N. S. Sariciftci, T. Fromherz, M. T. Rispens, L. Sanchez and J. C. Hummelen, *Adv. Funct. Mater.*, 2001, **11**, 374-380.
25. Y. He, H.-Y. Chen, J. Hou and Y. Li, *J. Am. Chem. Soc.*, 2010, **132**, 1377-1382.
26. H. Zhou, L. Yang, A. C. Stuart, S. C. Price, S. Liu and W. You, *Angew. Chem. Int. Edit.*, 2011, **50**, 2995-2998.
27. H. Xin, S. Subramaniyan, T.-W. Kwon, S. Shoaee, J. R. Durrant and S. A. Jenekhe, *Chem. Mater.*, 2012, **24**, 1995-2001.
28. X. Guo, M. Zhang, L. Huo, C. Cui, Y. Wu, J. Hou and Y. Li, *Macromolecules*, 2012, **45**, 6930-6937.
29. T. Ameri, T. Heumueller, J. Min, N. Li, G. Matt, U. Scherf and C. J. Brabec, *Energy Environ. Sci.*, 2013, **6**, 1796-1801.
30. H. Y. Chen, J. H. Hou, S. Q. Zhang, Y. Y. Liang, G. W. Yang, Y. Yang, L. P. Yu, Y. Wu and G. Li, *Nat. Photonics*, 2009, **3**, 649-653.
31. D. Dang, W. Chen, R. Yang, W. Zhu, W. Mammo and E. Wang, *Chem. Commun.*, 2013, **49**, 9335-9337.
32. T. S. van der Poll, J. A. Love, N. Thuc-Quyen and G. C. Bazan, *Adv. Mater.*, 2012, **24**, 3646-3649.
33. Y. Zhang, S.-C. Chien, K.-S. Chen, H.-L. Yip, Y. Sun, J. A. Davies, F.-C. Chen and A. K. Y. Jen, *Chem. Commun.*, 2011, **47**, 11026-11028.
34. M. C. Scharber, M. Koppe, J. Gao, F. Cordella, M. A. Loi, P. Denk, M. Morana, H. J. Egelhaaf, K. Forberich, G. Dennler, R. Gaudiana, D. Waller, Z. G. Zhu, X. B. Shi and C. J. Brabec, *Adv. Mater.*, 2010, **22**, 367-370.
35. Murgatro.Pn, *J. Phys. D: Appl. Phys.*, 1970, **3**, 151-156.
36. G. H. Lu, H. W. Tang, Y. A. Huan, S. J. Li, L. G. Li, Y. Z. Wang and X. N. Yang, *Adv. Funct. Mater.*, 2010, **20**, 1714-1720.
37. S. Albrecht, S. Janietz, W. Schindler, J. Frisch, J. Kurpiers, J. Kniepert, S. Inal, P. Pingel, K. Fostiropoulos, N. Koch and D. Neher, *J. Am. Chem. Soc.*, 2012, **134**, 14932-14944.
38. A. C. Stuart, J. R. Tumbleston, H. Zhou, W. Li, S. Liu, H. Ade and W. You, *J. Am. Chem. Soc.*, 2013, **135**, 1806-1815.

Captions to Tables and Figures

Table 1. Optical, electrochemical properties and hole mobility of PDTSBT-F and PDTSBT.

Table 2. Photovoltaic performance of PDTSBT-F and PDTSBT devices.

Scheme 1. Synthetic route towards polymers PDTSBT-F and PDTSBT. (PDTSBT-F is a regiorandom polymer)

Figure 1. The UV−vis spectra of PDTSBT-F and PDTSBT (a) in CB solutions and (b) in films spin-coated from their CB solution, respectively.

Figure 2. CV curves of PDTSBT-F and PDTSBT films.

Figure 3. XRD profiles of PDTSBT-F and PDTSBT films spin-coated from their CB solutions on Si substrates.

Figure 4. (a) Hole-only I–V curves of PDTSBT-F and PDTSBT films. The inset shows a hole-only device structure. (b) linear fits for the plots of $\ln(I/V^2)$ versus $V^{1/2}$ based on the SCLC model.

Figure 5. (a) J–V characteristics and (b) IPCE of PDTSBT-F and PDTSBT devices processed with $PC_{71}BM$.

Figure 6. XRD profiles of PDTSBT-F/$PC_{71}BM$ and PDTSBT/$PC_{71}BM$ composite films on PEDOT:PSS-coated Si substrates.

Figure 7. TEM of PDTSBT (a) and (b) PDTSBT-F composite films with $PC_{71}BM$, respectively.

1 Table 1. Optical, electrochemical properties and hole mobility of PDTSBT-F and PDTSBT.

Polymer	λ_{max} (nm) solution[a]	λ_{max} (nm) film	λ_{edge} (nm) film	E_g^{opt} (eV)	HOMO (eV)[b]	LUMO (eV)[b]	μ_h ($cm^2\ V^{-1}\ s^{-1}$)[c]
PDTSBT	670	760	850	1.46	-5.00	-3.20	5.54×10^{-5}
PDTSBT-F	670	750	840	1.48	-5.17	-3.26	1.09×10^{-4}

[a]Measured at 90 °C. [b]Measured by CV. [c]Measured by SCLC.

2

3

1 Table 2. Photovoltaic performance of PDTSBT-F and PDTSBT devices.

Active layer	J_{sc} (mA cm^{-2})	V_{oc} (V)	FF	PCE (%)
PDTSBT/$PC_{71}BM$ (CB)	14.35	0.64	0.51	4.68 (4.50)[a]
PDTSBT-F/$PC_{71}BM$ (CB + 1 vol % DIO)	15.96	0.70	0.60	6.70 (6.55)[a]

[a]Values in parentheses represent the average PCE from 60 devices.

2

3

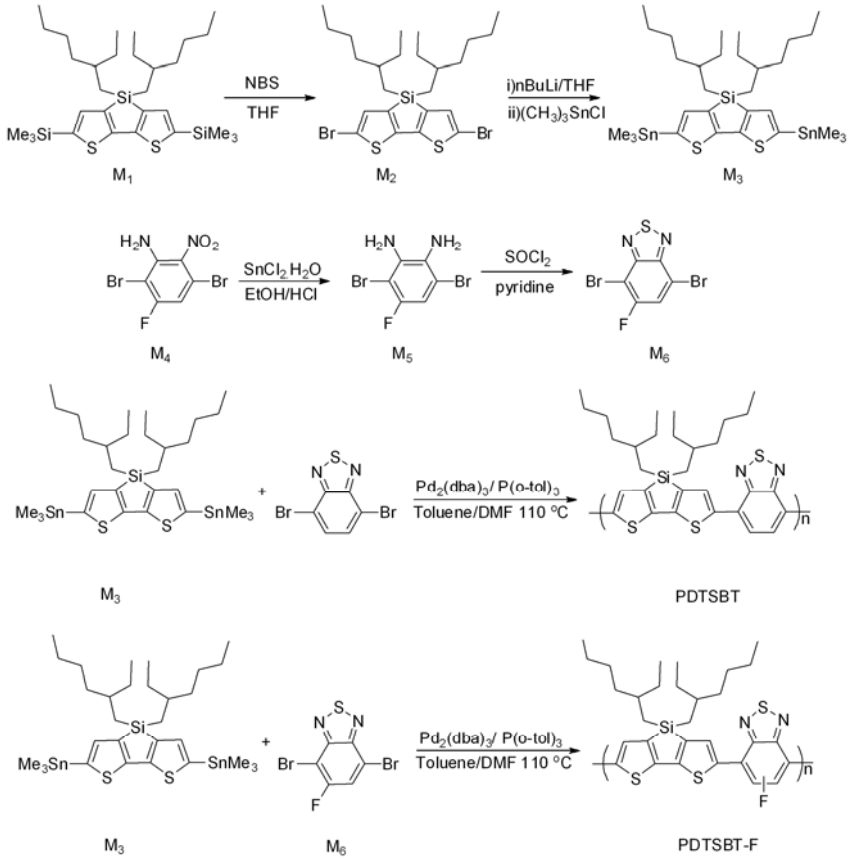

Scheme 1. Synthetic route towards polymers PDTSBT-F and PDTSBT. (PDTSBT-F is a regiorandom polymer)

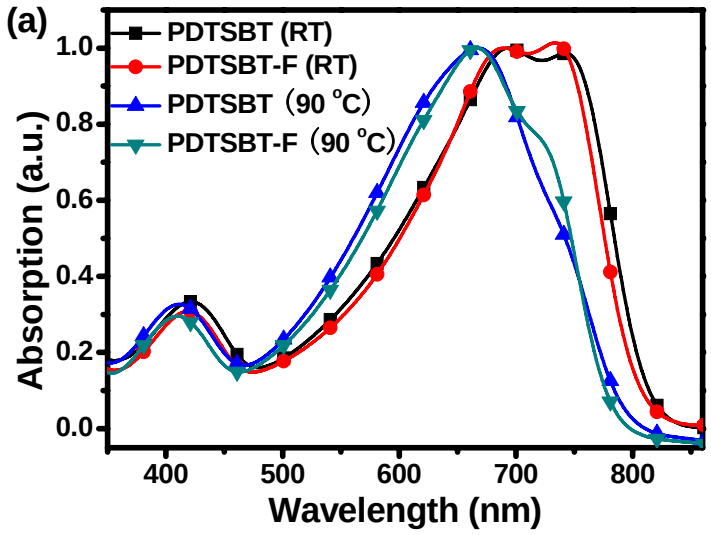

1

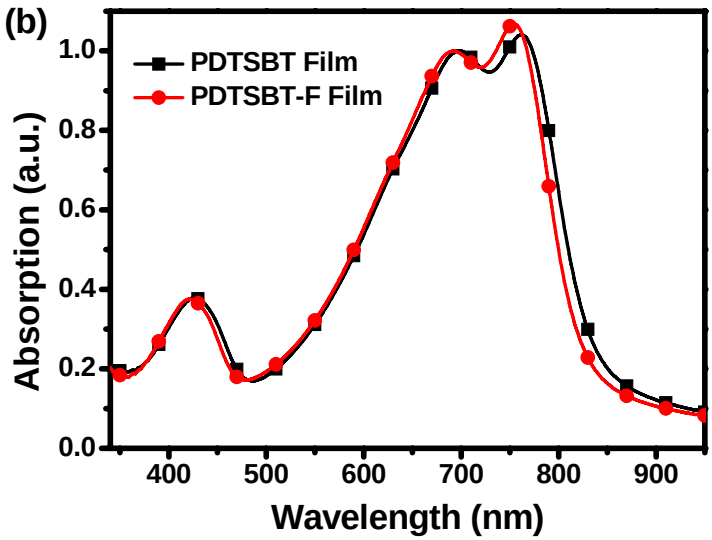

2

3 Figure 1. The UV−vis spectra of PDTSBT-F and PDTSBT (a) in CB solutions and (b) in films

4 spin-coated from their CB solution, respectively.

5

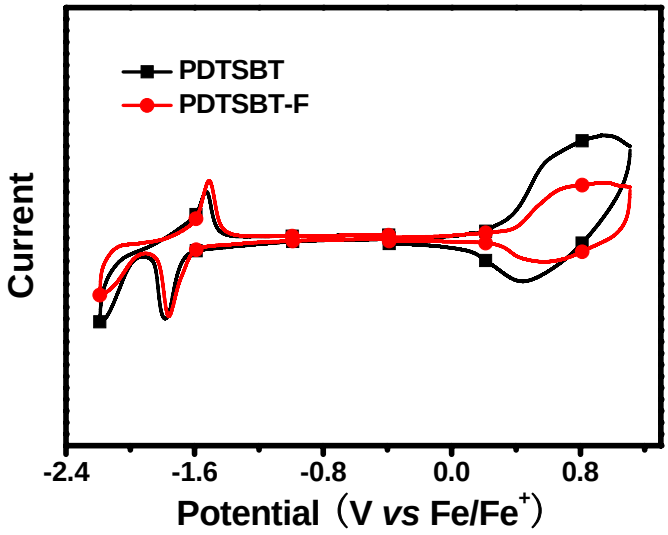

Figure 2. CV curves of PDTSBT-F and PDTSBT films.

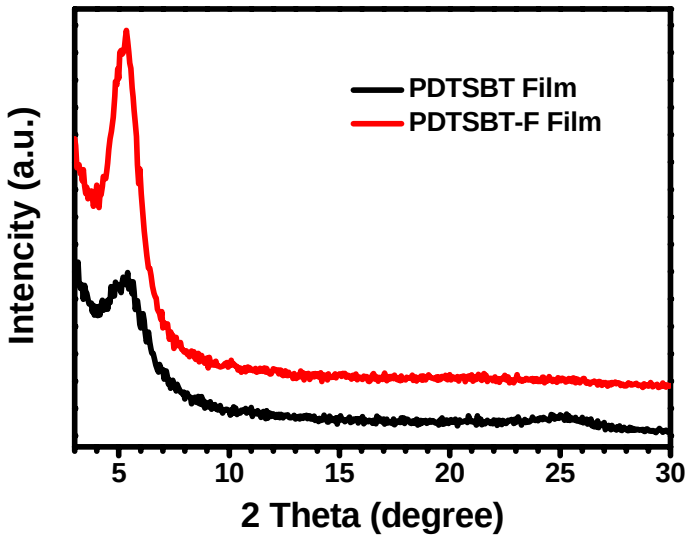

Figure 3. XRD profiles of PDTSBT-F and PDTSBT films spin-coated from their CB solutions on Si substrates.

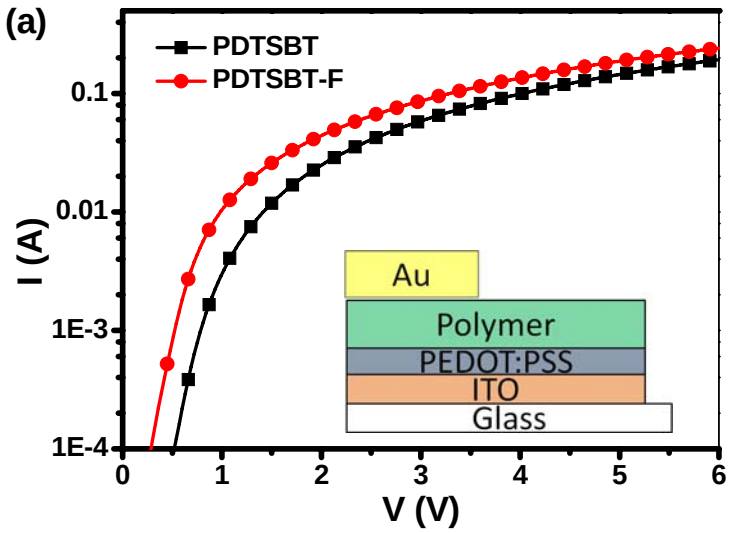

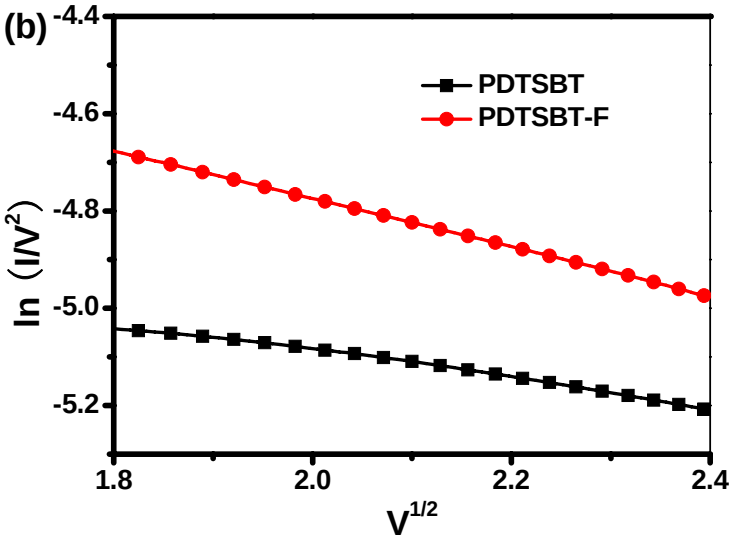

Figure 4. (a) Hole-only I–V curves of PDTSBT-F and PDTSBT films. The inset shows a hole-only device structure. (b) linear fits for the plots of $\ln(I/V^2)$ versus $V^{1/2}$ based on the SCLC model.

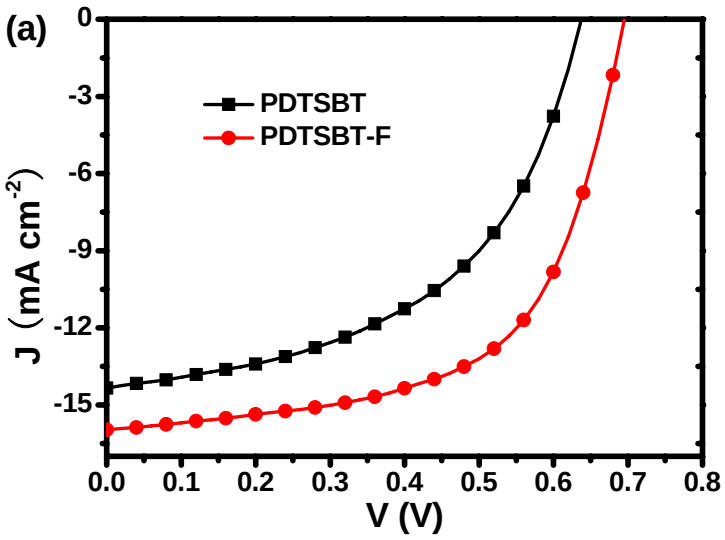

1

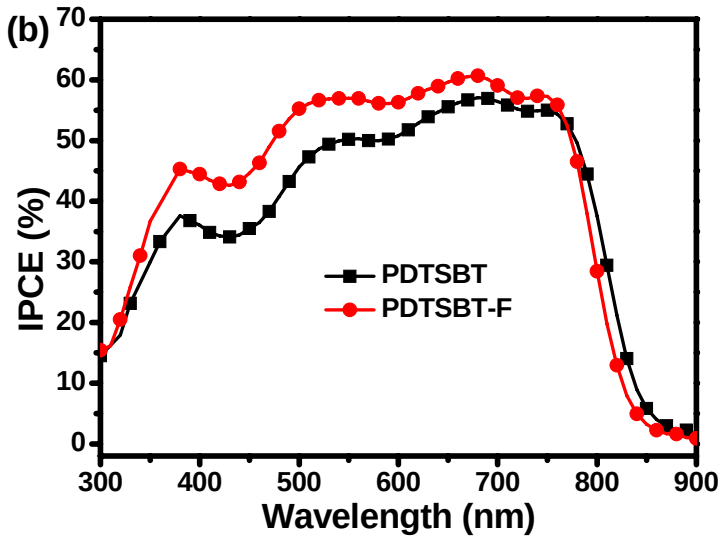

2

3 Figure 5. (a) J–V characteristics and (b) IPCE of PDTSBT-F and PDTSBT devices processed with

4 $PC_{71}BM$, respectively.

5

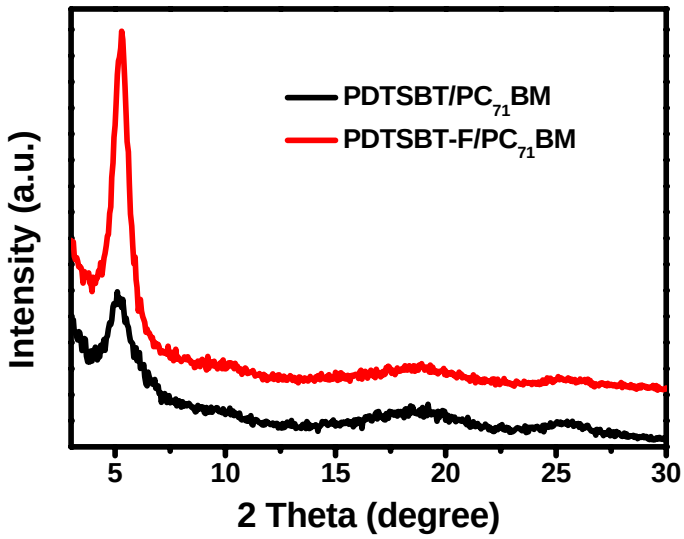

Figure 6. XRD profiles of PDTSBT-F/$PC_{71}BM$ and PDTSBT/$PC_{71}BM$ composite films on PEDOT:PSS-coated Si substrates.

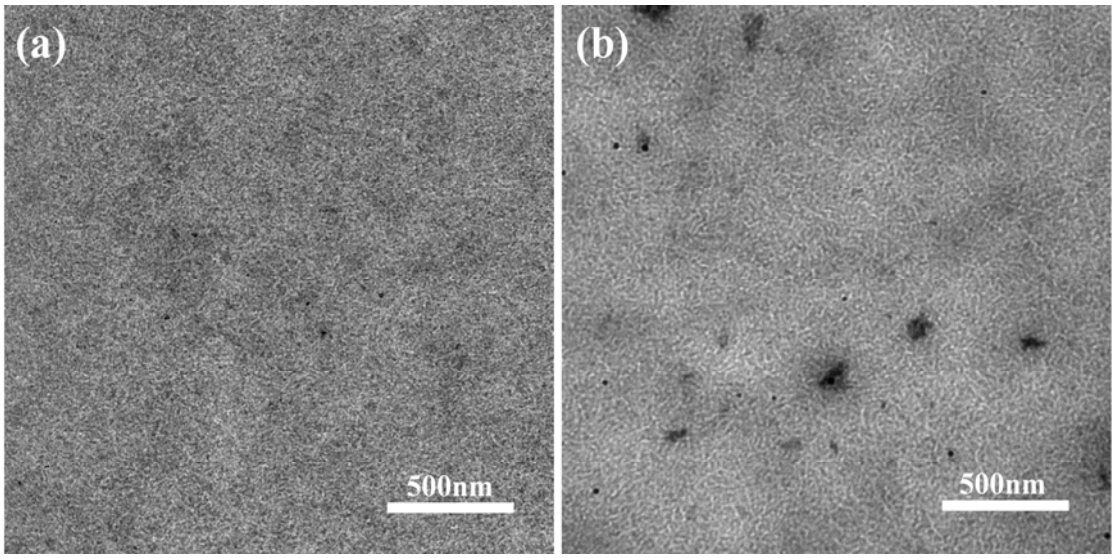

Figure 7. TEM of PDTSBT (a) and (b) PDTSBT-F composite films with $PC_{71}BM$, respectively.